© IJHG 2022 Int J Hum Genet, 22(3): 128-137 (2022)
PRINT: ISSN 0972-3757 ONLINE: ISSN 2456-6330 DOI: 10.31901/24566330.2022/22.03.814

Expression of Mutant Ectodysplasin-A Gene in Hypohidrotic Ectodermal Dysplasia

Fangqi He[1*], Hongfeng Wang[1, 2*], Shouyi Lu[2], Qingping Gao[2#], Feng Guo[2#], Ye Lei[2] and Tingwen Zeng[1]

[1]Department of Prosthodontics, Changsha Stomatological Hospital, Hunan Changsha 410004, China
[2]Department of Prosthodontics, Xiangya Hospital, Central South University, Hunan Changsha 410008, China

KEYWORDS Enzyme-linked Immunosorbent Method. Genetic Diagnosis. Prokaryotic Expression Vector. Protein Expression. Western Blot

ABSTRACT To investigate the protein expression changes of c.878T>G mutant and wild-type Ectodysplasin-A (EDA) gene on prokaryotic vectors from hypohidrotic ectodermal dysplasia (HED) families. The c.878T>G mutant and wild-type EDA genes were amplified, screened, and double-enzyme digested to obtain the target fragments. The recombinant plasmids were constructed and introduced into *Escherichia coli*. Lactosidase (IPTG) induces the expression of the target gene. The EDA protein expression content was determined by Western blot and enzyme-linked immunosorbent method. On the prokaryotic expression vector, the c.878T>G mutant and wild-type EDA protein expression increased with the increase of induction time, and the mutant protein expression was lower than the wild-type protein expression at the same point ($P<0.05$). In conclusion, the c.878T>G gene mutation in this family caused one amino acid of the EDA protein to become another amino acid, and the c.878T>G mutation site can lead to a significant decrease in the expression of EDA protein on the prokaryotic expression vector, is highly pathogenic and may be the cause of the HED family.

INTRODUCTION

Hypohidrotic ectodermal dysplasia (HED) is a congenital anomaly characterized by hypohydrosis, hypotrichosis and hypodontia (Khan et al. 2020; Anbouba et al. 2020). This type of syndrome affects the development of two or more ectodermal-derived organs, such as hair, teeth, nails, exocrine glands (Shwayder et al. 2019). The typical clinical manifestations are: sparse hair, loss of sweat glands, and abnormal tooth development (Liu et al. 2018). Ocular anomalies were less frequently observed, the most common ones being dysplasia of the lacrimal gland or meibomian gland that leads to dry eye and variable corneal involvement (Prat et al. 2021). Oral manifestations were mainly congenital absence of most teeth, or even complete edentulousness, which generally involved deciduous teeth and permanent dentition, and had a great impact on the physical and mental health of patients and seriously reduces the quality of life of patients.

During the development of human early embryos, Ectodysplasin-A (EDA) is gradually expressed in the epidermis of various parts of the embryo. As the embryonic development continues to improve, EDA begins to be expressed in hair follicles (Wu et al. 2019). The expression position of EDA in the embryonic development process had a certain connection with the clinical symptoms of HED patients, that is, the ectoderm-derived organs of HED patients were often congenital underdevelopment, such as sparse hair, missing teeth, missing nails or incomplete phenotypes (Wiœniewski et al. 2002; Mintoff et al. 2020; Wang et al. 2020). These studies indicated the close relationship between EDA and HED from the perspective of developmental biology. As a disease-causing gene, HED patients due to its mutation account for 95 percent of the total number of patients (Deshmukh and Prashanth 2012), including nonsense mutations, missense mutations, and small fragment deletions and other types of mutations.

[#]Address for correspondence:
Qingping Gao,
E-mail: qingpinggao12@163.com
Feng Guo,
E-mail: fengguo202109@163.com
Address: Department of Prosthodontics,
Xiangya Hospital, Central South University,
No.172 Xiangya Road, Kaifu District,
Changsha City, Hunan Province 410008
Telephone: (0731) 84327495; *Fax.* (0731) 84327495

The researchers' group collected 4 unrelated HED families in the early stage. Through complete clinical examination, the 4 probands all had typical clinical manifestations and were male patients. The family inheritance law conformed to the X chromosome recessive inheritance type. Gene sequencing results showed that all families had mutations in the EDA gene, and they were all different, including 2 point mutations (c.466C>T, c.878T>G) and 2 deletion mutations (c.663-697del, c.587-615del) (Lu et al. 2013). By comparing with the reported mutation sites, the point mutation (c.466C>T) in one family is a known pathogenic mutation (Monreal et al. 1998), and the remaining three mutation sites (c.878T>G, c.663-697del, c.587-615del) are new unknown mutations. The online gene prediction software SIFT and PolyPhen-2 were used to predict the conservation and pathogenicity of the mutation site c.878T>G, and the EDA gene mutation site p.L293R (c.878T>G) and p.T221fsX6 (c.663-697del) and p.P196fsX33 (c.587-615del) were found, which had strong amino acid conservation among different species, suggesting that during species evolution, this newly discovered 3 EDA gene mutation sites may be located in an important functional area of the coding gene. Evaluation of the pathogenicity of the mutation site c.878T>G indicated that the mutation site was theoretically highly pathogenic (He et al. 2018).

Objectives

In order to further study the difference in protein expression between the c.878T>G mutant and the wild EDA gene, prokaryotic expression vectors of EDA gene (c.878T>G) mutant and wild-type in HED were constructed, and induced recombinant plasmid expression in *E. coli*, laying an experimental foundation for exploring the molecular mechanism of HED pathogenicity.

MATERIAL AND METHODS

Test Specimen

The peripheral blood of one representative patient with EDA gene mutation (c.878T>G) and peripheral blood of one representative normal control were used in this study. Before study, two subjects signed informed consent.

Instruments and Reagents

ABI 2720 polymerase chain reaction (PCR) instrument (Applied Biosystems, USA), low-voltage power electrophoresis instrument (Bio-Rad, USA), Du-640 UV spectrophotometer (Beckman, Germany), gel imaging system (Bio-Rad, USA), multifunctional Microplate reader (Tecan, Australia), ultrasonic cell crusher (Ningbo Scientz Company, China), TRIzol reagent (Shanghai Bioengineering Co., Ltd., China), ampicillin (Wuhan Fuxin Chemical Co., Ltd. , China), Kit reverse transcription kit (Dalian Bao Biotechnology company, China), PCR kit (Dalian TaKaRa Company, China), DNA gel recovery kit (Shanghai Yili Co., Ltd., China), T4DNA ligase (NEB, USA), restriction enzyme BamHI (NEB, USA), restriction Endonuclease Sac (NEB, USA), DEPC (Beijing Dingguo Biotechnology Co., Ltd., China), DNA molecular marker (Beijing Tiangen Biotechnology Co., Ltd. , China), common plasmid kit (Beijing Tiangen Biotechnology Co., Ltd. , China), pTZ57R/ T cloning kit (Thermo Scientific, USA), isopropyl beta-D-thiogalactopyranoside (IPTG) (Gene Co., Ltd., Hong Kong, China), primary antibody diluent (Shanghai Beyotime Biotechnology Company, China), sodium dodecyl sulfate-polyacrylamide gel electrophoresis (SDS-PAGE) electrophoresis solution (Shanghai Beyotime Biotechnology Company, China), EDA primary antibody (Wuhan Boster Biological Technology Co., Ltd., China), HRP-labeled goat anti-rabbit secondary antibody (Wuhan Boster Biological Technology Co., Ltd., China), EDA Enzyme-linked immunosorbent assay (ELISA) (Wuhan Boster Biological Technology Co., Ltd., China), Tris base (Majorbio Co., Ltd., China) , DH5α competent cells (Beijing Tiangen Biochemical Technology Co., Ltd., China), pET-25b(+) plasmid (Thermo Fisher Scientific, USA), E.coli BL21 (Beijing Tiangen Biochemical Technology Co., Ltd., China).

Peripheral Blood Sample Collection and Total RNA Extraction

Blood from patients with EDA gene mutations (c.878T>G) and normal control were collected, and placed in 2% EDTA anticoagulation tubes. The basic patient information was registered. According to the instructions of TRIzol

Reagent, total RNA from all subjects were extracted, and RNA integrity and concentration were detected by 1 percent agarose gel electrophoresis.

RNA Reverse Transcription

According to the reverse transcription kit instructions, reverse transcription was performed at 37°C for 15 min, the reverse transcriptase was inactivated at 85°C for 5 s, and held at 4°C to reverse transcription of mRNA into cDNA.

PCR Amplification of Wild-Type Gene Fragments

The reaction system included 10 μL ExTaq, 1 μL wild-type EDA cDNA ,1 μL F-EDA Primer(10 μM), 1 μL R-EDA Primer(10μM), and 7 μL ddH_2O. After the reaction system was prepared, the liquid was concentrated at the bottom by instant centrifugation. The PCR amplification conditions were:

Pre-denaturation at 94°C for 2 min, 35 cycles (94°C for 30s, 55°C for 30s, 72°C for 45s), 72°C extension for 5 min.

Overlap PCR Site-directed Mutation of EDA Gene

Log in to University of California Santa Cruz (UCSC) Genome Brower, query the human EDA gene sequence, design specific primers. The primers were synthesized by BGI Genomics, China. The primers F-EDA (ATCGGATCCATGGGCTACCCGGAGG) and R-EDA (GACAAGCTTCTAGGATGCAGGGGCTTC) were specific primers at both ends of the EDA gene. Among them, the primers F-M-EDA (AGCGGGGAGCG (mutation site) GGAGGTACTG) and R-M-EDA (CAGTACCTCCC (mutation site) GCTCCCCGCT) were intermediate primers. PCR amplification with F-EDA and RM-EDA, R-EDA and FM-EDA was performed to obtain PCR products from the upper and lower ends respectively. The products at both ends are recovered and mixed to make each other as template and primer. The overlapping PCR was performed by using this product as a template, primers (F-EDA and R-EDA) were added for amplification to obtain the full mutant gene. PCR amplification conditions are: 94^{0}C pre-denaturation for 2 min, 35 cycles (94^{0}C 30 s, 55^{0}C 30 s, 72^{0}C 45 s), 72^{0}C extension for 5 min.

Target Gene Cloning

After the above PCR products were detected by 1 percent agarose gel electrophoresis, the target DNA fragments were recovered and purified, and connected to the ready-to-use cloning vector pTZ57R/T, and transformed into DH5β competent cells. The blue protein screening on penicillin (Amp, 100 ìg/mL) plates was performed, white colonies were picked. After PCR and restriction enzyme digestion, sequence was performed to determine positive clones.

Construction of Prokaryotic Expression Vector

The positive clone product and the pET-25b(+) vector plasmid were double-enzyme digested with BamHI and SacI, respectively, and the target gene fragment was ligated with the expression vector (16°C, 10h) after digestion, and then transformed into DH5α competent cells by the ligation system. The transformed product was spread on LB solid agar medium containing ampicillin (100 μg/mL) and cultured in a 37°C incubator for 16 hours to obtain a prokaryotic expression vector containing the target gene. After identification by PCR and restriction enzyme digestion, it was transformed into the host strain *E. coli* BL21 for expression.

Target Protein Expression Induced By IPTG and Determination of Total Protein Concentration

A cloned strain was selected from the petri dish, inoculated on LB solid medium containing ampicillin (100 ìg/mL), and cultured at 37°C, and induced time gradient. After culturing for 4h, IPTG (final concentration 0.5 μg/mL) was added to induce the expression of the target protein, the induced bacteria solution at 0h, 1h, 2h, 3h, 4h, and 5h were taken and centrifuged at 6000r/min for 30S. The bacteria were collected. After washing, PBS was added to resuspend the bacteria solution, broken with ultrasound, centrifuged at 4^{0}C, 12000r/min for 10 min, and the supernatant was taken. The protein standard solution was prepared and diluted, sample was added, and it was detected by multifunctional microplate reader with the absorbance at 562 nm wavelength. The standard curve was drawn with absorbance as the x-axis and concentration as

the y-axis, and the concentration of the target protein was calculated based on the standard curve and the absorbance of the target protein.

Western Blot to Detect the Expression of EDA Protein

After measuring the total protein concentration of the supernatant, the sample volume of each sample was adjusted to unify the total protein loading volume of 20 μg, separated by 10 percent SDS-PAGE, and transferred to polyvinylidene fluoride (PVDF) membrane, incubated with EDA antibody (1:300 dilution) on a horizontal shaker overnight at 4°C, and washed. PVDF membrane and horseradish peroxidase-labeled goat anti-rabbit IgG were incubated at 37°C for 2h. ECL luminescence was performed, the film was placed in the film press box for development, the developer and fixer kit were used to prepare the developer and fixer for manual washing, the film was dried, and scanned. β-actin served as an internal control.

ELISA Method to Detect the Expression of EDA Protein

The supernatant of the sample after sonication was centrifuged. Total of 25 μL each of the antibody standard solution diluted according to the required multiples and the sample to be tested were added into the wells of the sample to be tested, and incubated at 37°C for 90 min. After washed, 100 μL of diluted biotin anti-human EDA antibody working solution according to the instructions (except tetramethylbenzidine (TMB) blank chromogenic wells) were added, sealed, incubated at 37°C for 60 min. After washed, 100 μL of ABC working solution (TMB blank chromogenic wells were excluded) were added, incubated at 37°C for 30 min and then washed the plate again, and added 90 ìL of TMB chromogenic solution in order, avoiding light for 15-20 min (depending on the color development situation), then added 100 μL of TMB stop solution, immediately measured the absorbance of the specimen on a 450 nm microplate reader, drew a standard curve, and calculated the sample concentration. The testing was carried out by the same operator to avoid human error and strict quality control.

Statistical Analysis

The SPSS19.0 statistical software was used for analysis. The difference in the mean between and within the group was analyzed by F test and independent sample test. The difference was statistically significant with a two-sided $P<0.05$, and the results were expressed as mean±standard deviation.

RESULTS

The bands of agarose gel electrophoresis were shown in the Figure 1, including three bands of 28S, 18S, and 5S. The brightness of 28S band was about twice of 18S band, and the bands were clear without dispersion phenomenon. The RNA concentration measured on the multifunctional microplate reader were between 300-2000 ng/μL, and the ratios of A260/A280 were between 1.8 and 2.1, indicating that the extracted RNA was of good quality without degradation or breakage.

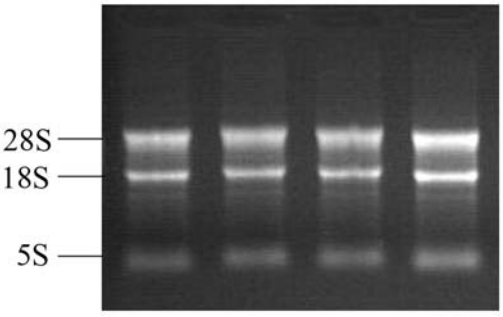

Fig. 1. Agarose gel electrophoresis of total RNA

PCR amplification products were detected by 1 percent agarose gel electrophoresis, the point mutations showed specific bands around 250 bp and 900 bp, and the target gene showed a specific band around 1000 bp, and the size was consistent with the theory value (Fig. 2).

One ml of the bacterial solution was sent to the sequencing company. The sequencing result was shown in Figure 3A. The clone containing the sequence of the target gene fragment was a positive clone. Subsequently, the recombinant plasmid verified by sequencing was extracted for double enzyme digestion, and the gene fragments were recovered. After detection by 1 percent agarose gel electrophoresis, a spe-

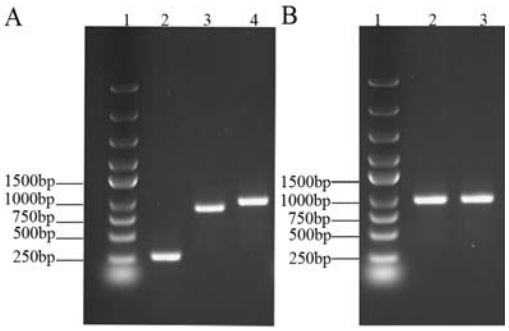

Fig. 2. (A) Agarose gel electrophoresis of the fragment before and after the mutation site c.878T>G amplified by PCR and the amplified fragment of wild-type EDA, note: 1: 250bp DNA marker, 2: Fragment 298bp after the mutation site, 3: Fragment 878bp before mutation site, 4: wild-type EDA 1176bp; (B) EDA-PCR agarose gel electrophoresis, note: 1: 250bp DNA marker, 2: mutant EDA fragment, 3: wild-type EDA fragment

cific band was shown near 1000 bp, and the size was consistent with the theoretical value (Fig. 3B).

he double enzyme digestion detected by 1 percent agarose gel electrophoresis showed bands with the same size as expected. The smaller band was about 1.2Kb and the larger band was about 5.2Kb, indicating that the target gene had been successfully inserted into the prokaryotic expression carrier (Fig. 4).

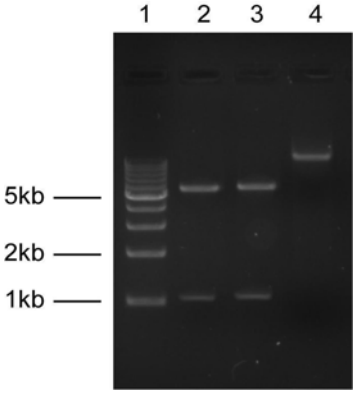

Fig. 4. Agarose gel electrophoresis diagram of EDA-pET-25b(+) double digestion
Note: 1: 1kb DNA marker; 2: mutant EDA-pET-25b(+) double digestion; 3: Wild-type EDA-pET-25b(+) double enzyme digestion; 4: pET-25b(+) empty plasmid control

Protein Expression Induced by IPTG

IPTG-induced bacterial solution for 1h, 2h, 3h, 4h, and 5h were detected by SDS-PAGE, and results showed that the expression of the target protein gradually increased and tended to stabi-

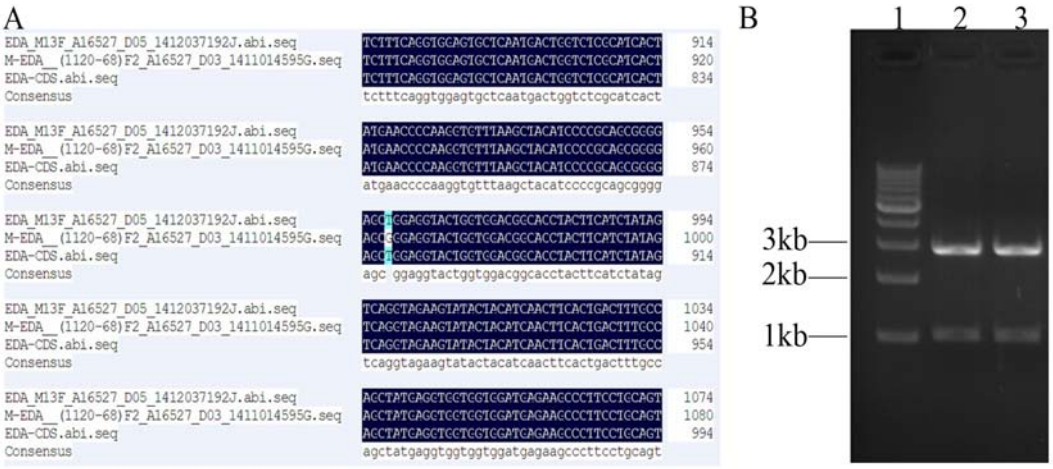

Fig. 3. (A) Sequencing comparison map of EDA-pTZ57R/T plasmid
(B) Agarose gel electrophoresis of EDA-pTZ57R/T double enzyme digestion,
Note: 1: 1kb DNA marker; 2: mutant EDA-pTZ57R/T double digestion; 3: wild-type EDA-pTZ57R/T double digestion

lize, and the difference between the expression of each group protein before the induction was statistically significant (P<0.05), indicating that the researchers' induced expression was successful (Fig. 5). The mutant EDA protein began to be expressed at a later time, and the expression was significantly lower than the wild-type EDA protein at the same point. The difference between the two groups was statistically significant (P<0.05) (Table 1).

Wild-type and Mutant EDA Protein Detected by Western Blot

The results showed that the expression of wild-type and mutant EDA protein gradually increased and stabilized with the increase of induction time, and the difference was statistically significant compared with the expression of each group before induction (P<0.05). The mutant EDA protein began to be expressed at a later time, and the expression level was significantly lower than that of the wild-type EDA protein at the same point. The difference between the groups was statistically significant (P<0.05) (Table 2).

Wild-type and Mutant EDA Protein Detected by ELISA

In order to further verify the results of Western blot, ELISA was used to analyze the expression products, and relatively accurately showed the differences in expression levels when differ-

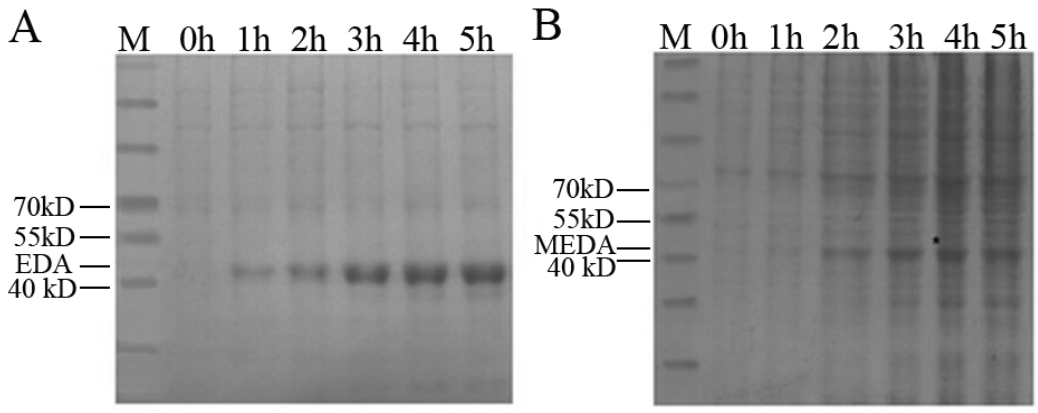

Fig. 5. SDS-PAGE electrophoresis diagram of the expression product of the prokaryotic expression vector induced by IPTG.
(A) Wild type EDA expression vector;
(B) Mutant EDA expression vector

Table 1: Total protein optical density values of wild type and mutant type expression vectors at different time points (±s)

Groups	*N*	*Optical density values of IPTG*						*P[a] value*
		0h	*1h*	*2h*	*3h*	*4h*	*5h*	
EDA	3	593.6±37.7	3745±237.9	4817.2±132.8	6962.8±442.2	9085.7±577.0	9195.5±584.0	0.000
M-EDA	3	498.6±31.7	697.9± 44.3	2597.6±165.0	2964.4±188.2	3408.4±216.5	3625.2±230.2	0.000
F value		0.101	4.280	0.093	1.867	2.290	2.124	
P[b] value		0.029	0.000	0.000	0.000	0.000	0.000	

Note: M-EDA meant mutant EDA, [a] meant P<0.05 when the optical density value of IPTG induced 1-5h in the same group was compared with that before induction, [b] meant P<0.05 when the optical density value at the same point was compared between different groups.

Table 2: Optical density of each band at different time points (±s) detected by Western blot

Groups	*N*	*Optical density values of IPTG*						*P[a] value*
		0	*1*	*2*	*3*	*4*	*5*	
EDA	3	570.9±48.4	4304.1± 364.8	5627.0±477.0	6342.7±537.6	6550.2± 555.2	6925.7±587.1	
M-EDA	3	189.7±11.4	1727.0± 104.1	2020.4±121.8	3938.9±237.5	4039.9± 243.6	4758.1±286.9	
F value		2.420	2.057	2.275	1.105	1.120	0.881	
P[b] value		0.000	0.000	0.000	0.002	0.002	0.005	

Note: M-EDA meant mutant EDA, [a] meant P<0.05 when the optical density value of IPTG induced 1-5h in the same group was compared with that before induction, [b] meant P<0.05 when the optical density value at the same point was compared between different groups

ent time gradients were induced. The results showed that with the increase of the induction time, the expression of the target protein gradually increased, and the expression of the mutant EDA protein was significantly lower than the expression of the wild-type EDA protein at the same time, the difference was statistically significant (P< 0.05) (Table 3).

DISCUSSION

The EDA gene is a pathogenic gene for hypohidrosis-type ectodermal hypoplasia. The EDA protein is a type II transmembrane protein and has multiple subtypes (EDA-A1 and EDA-A2 are the most common and longest subtypes), which mainly mediates signal transduction between epidermis and mesenchyme and between cells (Rasouliha et al. 2018). As an important member of the tumor necrosis factor ligand family, EDA protein has been fully studied in the field of developmental biology (Podzus et al. 2017). EDA was recently identified as a liver-secreted protein that is increased in the liver and plasma of obese mice and causes skeletal muscle insulin resistance (Bayliss et al. 2021). It can regulate the morphogenesis of the body and maintain the development of ectoderm-derived organs such as teeth, hair, sweat glands and other skin accessory organs (Xue et al. 2019) .This study found that the c.878T>G mutation family belonged to the clinical family, and the proband's nephew and cousin had similar behaviors. Genetic testing showed that base at position 878 of exon 7 of the EDA gene was changed from thymine to guanine, and the code was changed from CTG to CGG, resulting in the encoded amino acid at position 293 changed from leucine to arginine (p.Leu293Arg). It was confirmed from the genetic level that this mutation is the cause of ectoderm hypoplasia in this family. It is found that this mutation site is located in the TNF family ligand domain composed of 150 amino acids at the C-terminus of the EDA gene, and is one of the four important functional regions of the EDA gene (Christine and Schneider 2014), and its main function is to mediate specific binding to the receptor EDAR. Mutations in this region affect the binding of EDA protein to receptor EDAR, and fail to activate the NF-κB

Table 3: Protein expression of each group at different time points (pg/ml, ±s) detected by ELISA

Groups	*N*	*Protein expression at each point of induction of IPTG*						*P[a] value*
		0h	*1h*	*2h*	*3h*	*4h*	*5h*	
EDA	3	3.97±0.28	116.31±0.30	123.36±3.08	161.22±3.84	225.18±5.51	238.65±3.21	0.000
M-EDA	3	2.70±0.40	92.04±0.40	101.99±2.41	119.25±0.98	164.04±1.58	181.22±3.64	0.000
F value		0.632	0.326	0.515	6.395	6.976	0.049	
P[b] value		0.011	0.000	0.001	0.000	0.000	0.000	

Note: M-EDA meant mutant EDA, [a] meant P<0.05 when the protein expression of IPTG induced 1-5h in the same group was compared with that before induction, [b] meant P<0.05 when the protein expression at the same point was compared between different groups.

signaling pathway, leading to defects in the development of tissues and organs derived from ectoderm. NF-κB signaling pathway has been recognized as a classic signaling pathway related to HED (Smahi et al. 2002; Clauss et al. 2008).

In order to study the function of the protein, the researchers' must first obtain the expression of the target protein under in vitro conditions. At present, the foreign gene expression target protein mainly has two expression systems, prokaryotic and eukaryotic. Among them, the prokaryotic expression system is the first to be adopted and the research is the most mature. Compared with eukaryotic expression systems, it has the advantages of low price, efficient and fast expression, and easy purification, and is widely used in bioengineering. However, the prokaryotic expression system lacks the post-translational processing and modification process of eukaryotic proteins, thus losing part of the protein activity, and the expressed protein often forms inclusion bodies and is not easy to purify and separate, it is often used in basic research (Garcia et al. 1993). The *E. coli* expression system is the host most used for foreign genes to express the target protein (Terol et al. 2021). Therefore, the classic pET system was chosen in the prokaryotic expression system, pET-25b (+) as the expression vector, with a total length of 5547bp, which can obtain high-efficiency transient expression in *E. coli.*

The pCMV-EDA-A1 and pGEX-4T-3 plasmids were digested by Sma I and Xho I and then ligated, and identified by EcoRI digestion, the EDA gene prokaryotic expression vector pGEX-4T-3-EDA was successfully constructed, induced by IPTG, and the supernatant was taken, SDS-PAGE electrophoresis detection showed that a specific band was seen at 49KD, and the protein expression increased slightly with the increase of induction time (Gan et al. 2003). The results were consistent with this result. The pET-25b(+)-W/M-EDA recombinant plasmid was successfully constructed and induced the recombinant plasmid to express efficiently in prokaryotic cells, proving that the EDA gene induced in vitro can be obtained in prokaryotic cells.

Constructing an animal model of HED will help us further understand the pathogenesis of the disease and provide a reference for clinical treatment. As a very common biological model, mice have some genetic diseases that are surprisingly similar to humans, and HED is a typical type. The pathogenic gene Ta of Tabby disease in mice is highly similar to EDA in humans (Mandy et al. 2018; Risnes et al. 2005). During the embryonic development of normal mice, the expression of Ta can be detected in the teeth, skin epithelium and its accessory organs, but Tabby mice do not express. When the mouse EDA-A1 subtype gene was transferred to Tabby mice through transgenic technology, some skin appendages of male Tabby mice began to develop, and the growth of their hair, dermis, sweat glands, and molar teeth were almost completely restored (Srivastava et al. 2001) , the number of hair follicles can even approach the normal level. Study had confirmed that pregnant Tabby mice were treated with recombinant EDA-A1, the molecule can enter the mouse embryo through the placental barrier, thereby improving the Tabby phenotype of the mouse after birth, including the normalization of sweat gland development (Gaide and Schneider. 2003). Srivastava et al. (1997) observed the expression of Ta gene in normal mice by in situ hybridization with a labeled reverse RNA probe, and the results showed that Ta can be detected in the epidermis within 14 days (E14) of mouse embryos. Early postnatal treatment with EDA1 leading to delayed hair follicle formation attenuated the kink, and Tabby mice born after prenatal administration of EDA1, however, showed normal tail skin proliferation, no signs of kinking and, interestingly, a normalized vertebral bone density (Kossel et al. 2021). On the contrary, Tabby mice deficient in Ta gene is highly homologous to human EDA gene, it is not expressed in the affected tissues and organs.

Montonen et al. (1998) studied the expression and location of various spliceosome of EDA gene and found that EDA-A1 and EDA-A2 were expressed in human liver, brain, kidney, heart, lung, pancreas, skeletal muscle and placenta. But the expression level was low. The above results showed that although the expression level of EDA gene was very low, it was essential to maintain the formation and function of ectoderm-derived skin and its accessory organs. This experiment also confirmed that under the same induction conditions, the expression of mutant EDA protein was significantly lower than that of wild-type, indicating that the mutation had a signifi-

cant impact on the expression of EDA gene, leading to the occurrence of ectodermal hypoplasia in the proband, which was also corroborated the previous prediction of its pathogenicity.

CONCLUSION

The c.878T>G gene mutation in this family caused one amino acid of the EDA protein to become another amino acid, which may cause changes in the folding and spatial structure of the EDA protein during translation and processing, and affect the binding and transportation of the EDA protein to its receptor, resulting in different clinical manifestations. The specific mechanism remains to be further studied in order to achieve the purpose of guiding clinical treatment.

RECOMMENDATIONS

In the next step, the researchers' will transfect eukaryotic cells related to tooth development, and further explore the effect of mutant EDA genes on ectoderm-derived tissues and organs from the protein level.

AUTHORS CONTRIBUTIONS

Fangqi He and Hongfeng Wang carried out the studies, participated in collecting data, and drafted the manuscript, they are both first joint Authors. Shouyi Lu and Qingping Gao performed the statistical analysis and participated in its design. Feng Guo and Ye Lei, Tingwen Zeng helped to draft the manuscript and performed the data analysis. All authors read and approved the final manuscript.

REFERENCES

Anbouba GM, Carmany EP, Natoli JL 2020. The characterization of hypodontia, hypohidrosis, and hypotrichosis associated with X inked hypohidrotic ectodermal dysplasia: A systematic review. *American Journal of Medical Genetics*, 182(4): 831-841.

Bayliss J, Ooi GJ, Nardo WD, Shah Y, Watt MJ 2021. Ectodysplasin A is increased in non-alcoholic fatty liver disease, but is not associated with type 2 diabetes. *Frontiers in Endocrinology*, 12: 642432.

Christine KQ, Schneider P 2014. Ectodysplasin A (EDA) – EDA receptor signalling and its pharmacological modulation. *Cytokine & Growth Factor Reviews*, 25(2): 195-203.

Clauss F, Manière MC, Obry F, Waltmann E, Hadj-Rabia S, Bodemer C, Alembik Y, Lesot H, Schmittbuhl M 2008. Dento-craniofacial phenotypes and underlying molecular mechanisms in hypohidrotic ectodermal dysplasia (hed): A review. *Journal of Dental Research*, 87(12): 1089-1099.

Deshmukh S, Prashanth S 2012. Ectodermal dysplasia: A genetic review. *International Journal of Clinical Pediatric Dentistry*, 5(3): 197-202.

Gaide O, Schneider P 2003. Permanent correction of an inherited ectodermal dysplasia with recombinant EDA. *Nature Medicine*, 9(5): 614-618.

Gan Y, Wang Z, Chen S 2003. Expression of EDA gene in prokaryotic cells. *Journal of Clinical Stomatology*, 4: 203-205.

Garcia A, van Duin J, Pleij CW 1993. Differential response to frameshift signals in eukaryotic and prokaryotic translational systems. *Nucleic Acids Research*, 21(3): 401-406.

He F, Wang H, Zhang X, Gao Q, Guo F, Chen C 2018. Conservation analysis and pathogenicity prediction of mutant genes of ectodysplasina. *BMC Medical Genetics*, 19(1): 209-216.

Khan SA, Rukan A, Ullah A, Bibi N, Kalsoom IU 2020. Homozygous variants of EDAR underlying hypohidrotic ectodermal dysplasia in three consanguineous families. *European Journal of Dermatology*, 30(4): 408-416.

Kossel CS, Wahlbuhl M, Sonia SM, Park J, Christine KQ, Michaela S, Klaus M, Schneider P, Schneider H 2021. Correction of vertebral bone development in Ectodysplasin A1-deficient mice by prenatal treatment with a replacement protein. *Frontiers in Genetics*, 12: 709736.

Liu N, Niu S, Cao XR, Cheng JQ, Gao SY, Yu XJ, Wang HD, Dong CS, He XY 2018. Let-7b regulates alpaca hair growth by downregulating ectodysplasin A. *Molecular Medicine Reports*, 17(3): 4688-4694.

Lu SY 2013. *EDA Gene Detection and Clinical Analysis in Families with Hypohidrosis Ectodermal Dysplasia*. Master's Thesis, Unpublished. Changsha: Central South University.

Mandy W, Sonia SM, Christine KQ , Angela D, Fahlbusch FB, Pascal S, Holm S 2018. Attenuation of mammary gland dysplasia and feeding difficulties in Tabby mice by fetal therapy. *Journal of Mammary Gland Biology & Neoplasia*, 23(3): 125-138.

Mintoff D, Pace N, Mercieca V, Bauer P, Borg I 2020. A novel c.916C>A EDA gene pathogenic variant in a boy with X linked hypohidrotic ectodermal dysplasia. *Clinical and Experimental Dermatology*, 46(3): 618-620.

Monreal AW, Zonana J, Ferguson B 1998. Identification of a new splice form of the EDA1 gene permits detection of nearly all X-linked hypohidrotic ectodermal dysplasia mutations. *The American Journal of Human Genetics*, 63(2): 380-389.

Montonen O, Ezer S, Saarialho-Kere UK, Herva R, Karjalainen-Lindsberg ML, Kaitila I, Schlessinger D, Srivastava AK, Thesleff I, Kere J 1998. The gene defective in anhidrotic ectodermal dysplasia is expressed in the developing epithelium, neuroectoderm, thymus, and bone. *Journal of Histochemistry*

& Cytochemistry Official Journal of the Histochemistry Society, 46(3): 281-289.

Podzus J, Kowalczyk-Quintas C, Schuepbach-Mallepell S, Willen L, Staehlin G, Vigolo M, Tardivel A, Headon D, Kirby N, Mikkola ML, Schneider H, Schneider P 2017. Ectodysplasin A in biological fluids and diagnosis of ectodermal dysplasia. *Journal of Dental Research*, 96(2): 217-224.

Prat DL, Katowitz WR, Strong A, Katowitz JA 2021. Ocular manifestations of ectodermal dysplasia. *Orphanet Journal of Rare Diseases*, 16(1): 197.

Rasouliha SH, Bauer A, Dettwiler M, Welle MM, Leeb T 2018. A frameshift variant in the EDA gene in Dachshunds with Xinked hypohidrotic ectodermal dysplasia. *Animal Genetics*, 49(6): 651-654.

Risnes S, Peterkova R, Lesot H 2005. Distribution and structure of dental enamel in incisors of Tabby mice. *Archives of Oral Biology*, 50(2): 181-184.

Shwayder T, Schneider SL, Icecreamwala D, Jahnke MN 2019. Hypohidrotic Ectodermal Dysplasia. *Journal of Glaucoma*, 28(4): 59-60.

Smahi A, Courtois G , Rabia SH , Döffinger R, Bodemer C, Munnich A, Casanova JL, Israël A 2002. The NF-κB signalling pathway in human diseases: From incontinentia pigmenti to ectodermal dysplasias and immune-deficiency syndromes. *Human Molecular Genetics*, 137(20): 567-581.

Srivastava AK, Durmowicz MC, Hartung AJ, Hudson J, Ouzts LV, Donovan DM, Cui CY, Schlessinger D 2001. Ectodysplasin-A1 is sufficient to rescue both hair growth and sweat glands in Tabby mice. *Human Molecular Genetics*, 26: 2973-2981.

Srivastava AK, Pispa J, Hartung AJ, Du Y, Ezer S, Jenks T, Shimada T, Pekkanen M, Mikkola ML, Ko MS, Thesleff I, Kere J, Schlessinger D 1997. The Tabby Phenotype is Caused by Mutation in a Mouse Homologue of the EDA Gene that Reveals Novel Mouse and Human Exons and Encodes a Protein (ectodysplasin-A) with Collagenous Domains. *Proceedings of the National Academy of Sciences of the United States of America*, 94(24): 13069-13074.

Terol GL, Gallego-Jara J, Martínez R, Vivancos AM, Díaz MC, Puente TD 2021. Impact of the expression system on recombinant protein production in Escherichia coli BL21. *Frontiers in Microbiology*, 12: 682001.

Wang X, Zhang ZY, Yuan S, Ren JB, Qu H, Zhang GZ, Chen WJ, Zheng SS, Meng LQ, Bai JP, Du QQ, Yang DR, Shen WJ 2020. A novel EDA1 missense mutation in X-linked hypohidrotic ectodermal dysplasia. *Medicine*, 99(11): e19244.

Wiœniewski S, Kobielak A, Trzeciak WH, Kobielak K 2002. Recent advances in understanding of the molecular basis of anhidrotic ectodermal dysplasia: Discovery of a ligand, ectodysplasin A and its two receptors. *Journal of Applied Genetics*, 43: 97-107.

Wu J, Cao J, Li C, Lu N, Wu J, Yan R, Zhang J, Zhang P, He X 2019. Expression of EDA and its receptor EDAR at dorsal hair follicles formation stage of embryonic mice. *Journal of Shanxi Agricultural University (Natural Science Edition)*, 39(4): 63-69. DOI: 10.13842/j.cnki.issn1671-8151.201812028

Xue YT, Liao BJ, Xie YJ, Li SY, Ma XY, Sun XF 2019. Establishment of an ectodermal dysplasia related gene EDA Knockout human embryonic stem cell line (WAe001-A-22) by CRISPR-Cas9 technology. *Stem Cell Research*, 34: 101379.

Paper received for publication in November, 2021
Paper accepted for publication in March, 2022